International Journal of Signal Processing, Image Processing and Pattern Recognition
Vol.9, No.11, (2016), pp.271-282
http://dx.doi.org/10.14257/ijsip.2016.9.11.25

A New Adaptive-Weighted Fusion Rule for Wavelet based PET/CT Fusion

R. Barani[1] and M. Sumathi[2]

[1]*Department of Computer Science, V.V.Vanniaperumal College for Women, Virudhunagar-626001, Tamil Nadu, India*
[2]*Department of Computer Science, Sri Meenakshi Government Arts College for Women, Madurai-625021, Tamil Nadu, India*
[1]*baranisrinivasan1994@gmail.com*,[2]*sumathivasagam@gmail.com*

Abstract

In recent years the Wavelet Transform (WT) had an important role in various applications of signal and image processing. In Image Processing, WT is more useful in many domains like image denoising, feature segmentation, compression, restoration, image fusion, etc. In WT based image fusion, initially the source images are decomposed into approximation and detail coefficients and followed by combining the coefficients using the suitable fusion rules. The resultant fused image is reconstructed by applying inverse WT on the combined coefficients. This paper proposes a new adaptive fusion rule for combining the approximation coefficients of CT and PET images. The Excellency of the proposed fusion rule is stamped by measuring the image information metrics, EOG, SD and ENT on the decomposed approximation coefficients. On the other hand, the detail coefficients are combined using several existing fusion rules. The resultant fused images are quantitatively analyzed using the non-reference image quality, image fusion and error metrics. The analysis declares that the newly proposed fusion rule is more suitable for extracting the complementary information from CT and PET images and also produces the fused image which is rich in content with good contrast and sharpness.

Keywords: *adaptive image fusion, fusion rule, image fusion, medical image fusion, PET/CT fusion, wavelet fusion*

1. Introduction

PET/CT is a multi-modality imaging technology increasingly used for diagnosis, staging and follow-up of several prominent diseases like malignancy, alzheimer’s disease and also to differentiate malignant from benign lesions. The basic principle of PET/CT imaging is the injection of a small quantity of biologically important material like glucose or oxygen which has been labeled with radio-nuclides containing a positron emitter, followed by the detection of emitted radiation using the detector, and the computation of a digital image that represents the distribution of the radiotracer in the body. The most commonly used radioactive substance in PET scan is FDG (fluorine-18 combined with deoxy-glucose) [1]. The metabolically active malignant cells have a higher absorption rate than the normal cells. So the emission of radiation from these cells is also higher and can be identified by the detectors. PET imaging offers the information about the metabolic changes in the tissues of the body, whereas, CT imaging provides fine details about structure, boundary and texture of hard tissues like bone and less detail about soft tissues. The dual modality imaging like PET/CT combines both the PET image and CT image and provides both the anatomic-metabolic information in a single image that can be useful for improved diagnostic assessment and treatment planning during the clinical activities.

Image fusion is the process of deriving a superlative image from two or more images of complementary nature. Recently, image fusion has been given greater importance in many applications, since it results in an image that is more valuable than any of the source images in terms of content and also free of redundancies and artifacts. Image fusion may be performed at three levels of image data: pixel level, feature level and decision level [2]. In pixel level, some mathematical calculations are performed on the intensity values of pixels of source image to obtain the fused image. At the feature level, the features like shape, edge, contrast, color, texture are first extracted from the source images and then the fusion is performed using the appropriate fusion rule. The decision level fusion operates on the symbolic representation of images for image fusion. These three levels of fusion can be performed either in the spatial representation or in the transform representation of an image. Pyramid representation and wavelet representation are primarily used for the multi-scale representation of an image.

Many image fusion algorithms such as simple average, maximum and minimum, median and rank, PCA, ICA, NMF, CCA, LDA and other HIS based algorithms [3] perform fusion operation on spatial information. These methods do not consider the multi-scale characteristics of an image and ~~results~~ in low contrast and blurring effects in the fused image. In transform representation, the fusion is performed by decomposing the images into multi-scale representation [4]. At the early stage of multi-scale image fusion, pyramid representation was adopted for image representation. Later, the wavelets have proven its ability in getting more directional information and well performed than pyramid based methods.

This paper proposes a new fusion rule Adaptive Weighted Average (AWA) for combining the approximation coefficients of PET and CT images. The adaptive weights are calculated based on the glucose absorption rate of metabolically active cells in the PET image. The efficiency of the newly proposed fusion rule is demonstrated by comparison with SA rule using the image information metrics EOG, SD and Shannon Entropy (ENT). The detail coefficients are combined using the existing rules such as absolute maximum (ABS-MAX), simple maximum (MAX), Window Based Verification Scheme (WBV) proposed by Li et.al and Weighted Average Scheme (WA) proposed by Burt et.al. The newly proposed adaptive fusion rule is compared with the simple average fusion rule for the various combinations of detail coefficient fusion rules ABS-MAX, MAX, WA and WBV. The resultant fused images are analyzed with non-reference image quality metrics Spatial Frequency (SF) and Entropy (ENT), non-reference image fusion metrics Fusion Factor (FF), Xydeas and Petrovic Measure ($Q^{(AB/C)}$) and Mutual Information (MI) and non-reference error metrics Perfect Fusion Error (PFE) [5,6]. The newly proposed Adaptive Weighted Average fusion rule [AWA] excels in quality, content and in suppression of errors than the Simple Average fusion rule [SA].

2. Overview of Wavelet Transform

A wavelet is a small wave that is used as tool to analyze transient, non-stationary or time-varying signals and is represented as $\psi(t)$. The Wavelet Transform (WT) [7] is the process of representing or expanding the signal $f(t)$ as the finite or infinite sum of real-valued expansion coefficients a_i and set of real-valued functions of t *i.e.*, $\psi(t)$ such that

$$f(t) = \sum_i a_i \psi_i(t) \tag{1}$$

If the expansion coefficients are unique, the set of real valued functions is called a basis. If the basis is orthogonal, the coefficients can be calculated by the inner product of real-valued function $\psi(t)$ with the signal $f(t)$ and is given by

$$a_i = \langle f(t), \psi_i(t) \rangle = \int f(t) \psi_i(t) dt \tag{2}$$

If the signal *f(t)* is a 2D function, WT for such a signal is constructed as a two-parameter system such that

$$f(t) = \sum_i \sum_j a_{i,j} \psi_{i,j}(t) \tag{3}$$

and the real-valued coefficients are obtained by the inner product of real valued function with the signal as follows:

$$a_{i,j} = \left\langle f(t), \psi_{i,j}(t) \psi_{i,j}(t) \right\rangle = \int f(t) \psi_{i,j}(t) dt \tag{4}$$

The 2D WT can be implemented by filtering followed by down-sampling the image with two separate filters, one in the horizontal direction and another in vertical direction. When 2D WT is applied on images, it results in four sub bands: HH, HL, LH and LL. The letter H represents the higher-order frequency and the letter L represents the lower-order frequency. Therefore, the decomposition of an image by WT at a particular level results in one lower-order frequency component and three higher-order frequency components. The LL sub band provides the coarse form an image which contains the base information, whereas the other sub bands contain the specific detail information such as edges and corners present in the image. The multi-resolution decomposition can be obtained by recursively applying the same process to the LL sub band and is represented in Figure1.

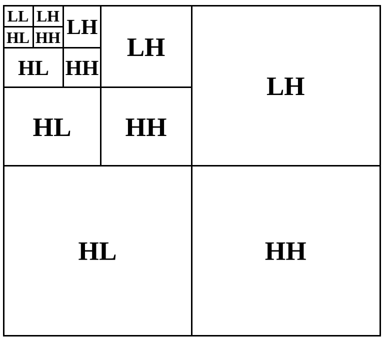

Figure 1. Multilevel Decomposition by Wavelet Transform

3. Image Fusion by Wavelet Transform

By considering WT as ω, inverse WT as ω^{-1}, the WT image fusion [8] is formally defined as:

$$I(i,j) = \omega^{-1}\Big(\phi\big(\omega(I_1(i,j)), \omega(I_2(i,j))\big)\Big) \tag{5}$$

Where, $I_1(i, j)$ and $I_2(i, j)$ are the two source images, $I(i, j)$ is the fused image and ϕ is the coefficient combination rule. The schematic diagram of wavelet based image fusion is illustrated in Figure 2.

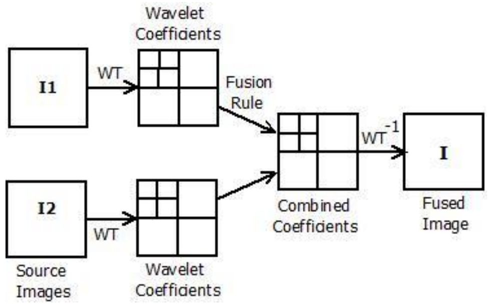

Figure 2. Schematic Diagram of Image Fusion using Wavelet Transform

The wavelet decomposition of an image results in one approximation coefficient component LL, and three detail coefficient components LH, HL and HH. Figure 3, shows the decomposed components of CT and PET images. In Figure 3, row1 shows the decomposed components of the CT image and row2 shows the decomposed components of the PET image. In both rows, the LL band contains the blurred version of the original content of an image, whereas the LH, HL and HH components holds the fine features such as edges and corners that are extracted from an image in three directions horizontal, vertical and diagonal.

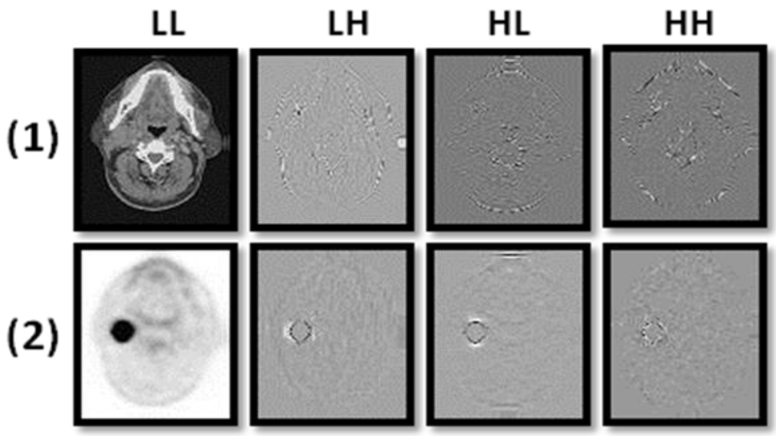

Figure 3. The LL, HH, LH and HL Components of CT/PET Data Set

3.1. Fusion Rules

The quality and the content of a fused image hardly depends on the selection of appropriate fusion rule. The unique rule is not appropriate for all the situations. The selection of the fusion rule mostly depends on the source and the nature of the input image. It also depends on the information present in the source image and the information needed in the fused image too. After decomposition, the approximation coefficients has the base content of the source image and the detail coefficients hold the prominent features of the source image like edges and corners. The fusion rule for approximation coefficients should look for combining all the basic information from both the images without any loss. At the same time, the fusion rule for detail coefficients should look for catching the most important features. Most commonly used fusion rules for combining the approximation and detail coefficients are discussed below:

By considering I_1 and I_2 as the two source images and I as the fused image, the coefficient combination rule ϕ is defined as

i) MAX rule: The MAX rule selects coefficients with largest magnitude and is given by

$$\phi(I_1, I_2) = I(i, j) = \max\left(I_1(i, j), I_2(i, j)\right) \tag{6}$$

where $i = 1$ *to* m and $j = 1$ *to* n. This rule can be used for combining the LL, LH, HL and HH sub bands of two images.

ii) ABS-MAX rule: The ABS-MAX rule selects the coefficients with largest absolute magnitude and is given by

$$\phi(I_1, I_2) = I(i, j) = \max\left(ABS(I_1(i, j)), ABS(I_2(i, j))\right) \tag{7}$$

where $i = 1$ *to* m and $j = 1$ *to* n. This rule can be used for combining the LL, LH, HL and HH sub bands of two images.

iii) Simple Average rule (SA): The SA rule computes the combined coefficients as the average of the coefficients of two images and is given by

$$\phi(I_1, I_2) = I(i, j) = \left(I_1(i,j)+I_2(i,j)\right)/2 \tag{8}$$

where $i = 1$ *to* m and $j = 1$ *to* n. This rule can be used for combining the all the four sub bands of two images.

iv) WA rule: The WA rule selects the coefficients based on the correlation between the two image's sub bands under the small window [9]. This method was proposed by PJ Burt et. al. and is given by

$$\phi(I_1, I_2) = I(i, j) = w_1(i, j) * I_1(i, j) + w_2(i, j) * I_2(i, j) \tag{9}$$

where w_1 and w_2 are the weights of two source images. The weights are calculated using the salience and match measure [9]. If the match measure is extremely varying, the weights are assigned with two extremes 0 and 1. On the other hand, the weights are hardly o.5 and 0.5.

ii) WBV rule: WBV uses an area based selection rule [10]. The decomposed component is separated into 3x3 or 5x5 windows. The salience measures, like variance or standard deviation, is measured over that window. In each window, if the measures of two images are close to each other, then the average rule is followed; otherwise the component with larger value is considered.

These fusion rules may be used for combining both the approximation and detail coefficients of both the source images.

3.2. Newly Proposed AWA Fusion Rule

In PET/CT image fusion, the approximation coefficients of CT image contain the anatomical information and approximation coefficients of PET image contain the metabolic information. When the anatomic information from CT image and the metabolic information from PET image are combined using the SA fusion rule [11-13], it will simply fade out both the information. On the other hand, if the fusion rule for combining the approximation coefficients of PET/CT image extracts only the pixels corresponding to metabolically active tissues from PET image and the pixels representing the anatomical information from a CT image, the fused image may retain both the anatomical information and metabolic information more clearly. Therefore, the weight should be adaptively calculated by considering either the pixel in the PET image is metabolically important or not. By considering the approximation coefficients of CT and PET images as

A_1 and A_2, the participation of each pixel for the fused image is determined by the adaptive weight and is calculated as

$$w(i,j) = \left(\max - A_2(i,j)) / \max\right) \tag{10}$$

where *w(i,j)* is the adaptive weight, *a(i,j)* is the approximation coefficient value of PET image at the position *(i,j)* and max is maximum intensity value of PET image. Then the fusion operation is performed as the adaptive-weighted average of approximation coefficients of two source images and is given by

$$A(i,j) = \left(A_1(i,j) * \left(1 - w(i,j)\right) + A_2(i,j) * w(i,j)\right) / 2 \tag{11}$$

where *A1(i,j)*, *A2(i,j)* and *A(i,j)* are the approximation coefficients of CT, PET image and the fused image.

The combined approximation coefficients should contain all the relevant information from both PET and CT image and also retains the contrast and sharpness of the source image. The effectiveness of the proposed fusion rule is shown by measuring the image information metrics Energy of Gradient (EOG), Standard Deviation (SD) and Shannon Entropy (ENT) on the combined approximation coefficients. If the value of the EOG is higher, the image shows better information. The SD measure the contrast of the image. The higher the contrast, clearer the image is. ENT is a statistical measure used to characterize the texture of an image.

4. Experimental Data and Analysis

The adaptive-weighted average wavelet fusion is experimented with Rider Lung PET/CT images available in The Cancer Imaging Archive (TCIA) database and with the scan real data for various combination rules. The simple average rule (SA) and adaptive weighted average (AWA) rule is adopted for combining the approximation coefficients. To combine the detail coefficients the maximum selection rule, absolute maximum rule, Weighted Average (WA) rule, and Window Based Verification (WBV) rules are used. The consistency check is per-formed for WA and WBV methods by considering the widow size as 3. The wavelet fusion is implemented with 'haar' wavelet and at the decomposition level is assumed as 1.

Since fused image should be both qualitatively and informatively rich, the resultant images are compared using the non-reference image quality metrics: SF, ENT, non-reference image fusion metrics: FF, $Q^{(AB/F)}$, MI and the non-reference error metrics: PFE. The SF measures the sharpness, ENT measures the information content in an image and FF, $Q^{(AB/F)}$, MI determines the amount of information extracted from the source images by measuring the correlation between the fused image and the source images and PFE measures the existence of artifacts and errors.

4.1. Data Set1

The data set 1 is the CT and PET images of an axial view of a neck of 39 yrs old patient and is shown in Figure 4. The size of both the images is 336 x 272 and is considered to be in 'jpeg' format.

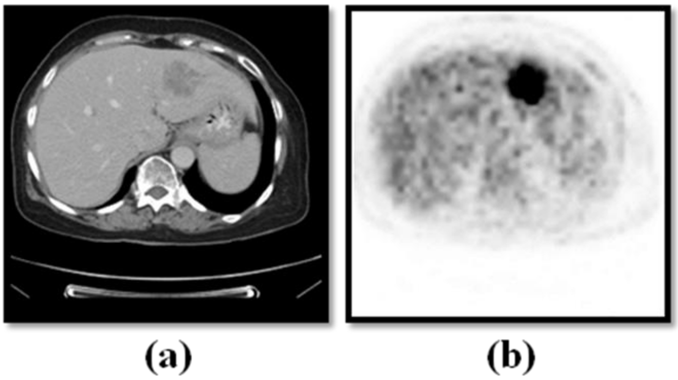

Figure 4. CT and PET Images of An Axial View of a Neck Showing the Necrotic Mass Lesion in the Base of Tongue

The CT image in Figure 4a, shows the shape, structure and boundaries of the different parts in the base of the tongue. The high intensity pixels represent hard tissues of bony structures, and the low intensity pixels represent the soft tissues. The PET image in Figure 4b, contains the information about the metabolic activity of the soft tissues, indicating the presence of necrotic mass lesion in the base of the tongue on left side extending to the left tonsillar fossa and to the parapharyngeal region which is not captured in the CT image. For the radiologist, if both the structural and the metabolic information is available in a single image, it is very useful for analyzing and localizing the malignant during diagnosis, treatment planning and staging.

4.2. Data Set2

Figure 5, shows the CT and PET images of an axial view of a neck of 63 yrs old male patient. The image size is 624 x 528 and is considered to be in 'jpeg' format. The CT image in Figure 5a, shows the shape, structure and boundaries of the bony structures of a neck. The PET image in Figure 5b, shows the metabolically active large mass lesion in the apicoposterior segment of right upper lobe with complete cut off the segmental bronchiole. For the radiologist, if both this complementary information is available in a single image, it is very useful for analyzing and localizing the malignant during diagnosis.

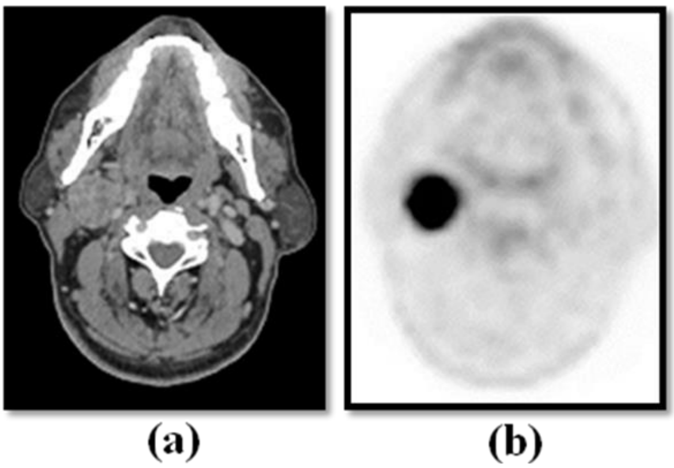

Figure 5. CT and PET Images of An Axial View of a Neck Showing Metabolically Active Large Mass Lesion in the Apicoposterior Segment of Right Upper Lobe

5. Results and Discussions

5.1. Data Set1

The LL sub bands of the PET and CT images of data set1 are shown in Figure 6a, and 6b. Figure 6c, and 6d, shows the combined approximation coefficients by using SA fusion rule and newly proposed AWA rule.

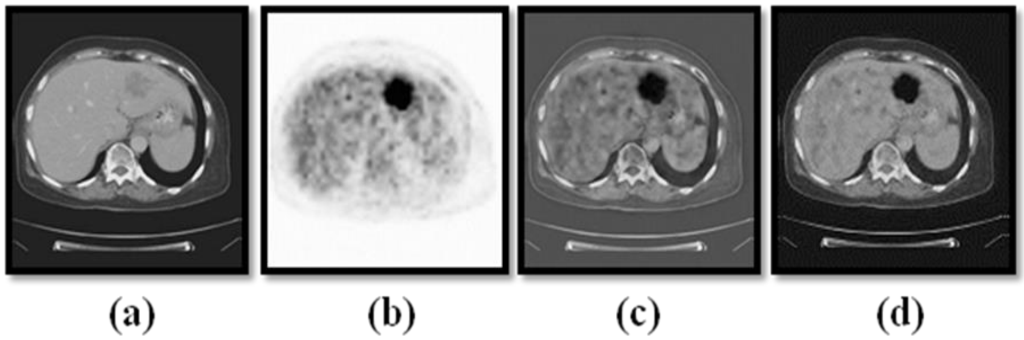

Figure 6. Data Set1 a) LL sub band of CT Image b) LL sub band of PET Image c) Fused Sub Band by SA Rule d) Fused sub Band by AWA Rule

In Figure 6c, it contains both the anatomic structures from 6a and metabolic information from 6b, but both the information are faded out. The contrast is suppressed and the entire image is not clear. Whereas the proposed AWA rule combines both the anatomic structures from 6a and metabolic information from 6b and also retains the contrast and clarity. The effectiveness of the proposed fusion rule is demonstrated by measuring the information content and clarity of the combined approximation coefficients by using the image information metrics Energy of Gradient (EOG), Standard Deviation (SD) and Shannon Entropy (ENT). If the value of the EOG is higher, the image shows better information. The SD measure the contrast of the image. The higher the contrast, clearer the image is. ENT is a statistical measure used to characterize the texture of an image. The values of EOG, SD and ENT for the fused approximation coefficients of the PET and CT images of data set 1 are given in Table 1.

Table 1. Estimation of EOG, SD and ENT for the Fused Approximation Coefficients of Data Set1

Fusion Rule	EOG	SD	ENT
SA	23129471	4.8768	29.4924
AWA	31320028	5.0528	55.1170

The proposed fusion rule AWA scores higher values for EOG, SD and ENT, which shows that it is superior in terms of information content and contrast for the fusion of approximation coefficients of the CT and PET images.

Figure 7, shows the resultant fused images of data set1 for WT based image fusion using different fusion rules. In Figure 7, the Figures 1a, 1b, 1c and 1d, are the output images obtained using SA rule for approximation coefficients and ABS_MAX, MAX, WA and WBV rules for detail coefficients respectively. In the same way, the Figures 2a, 2b, 2c and 2d are the output images obtained using AWA rule for approximation coefficients and ABS_MAX, MAX, WA and WBV rules for detail coefficients respectively.

From visual comparison, it is well known that the newly proposed adaptive weighted average rule extracts only the pixels of metabolically active tissues from the PET image and superimposed on the CT image. The detail coefficients that are combined by the fusion rules further add the clarity, sharpness and edges into the base content. Therefore, the fused image includes the metabolic information from the PET image and bony structures from CT image with boundaries, sharp edges and good contrast. Therefore, the newly proposed fusion rule performs well and is more suitable for the fusion of PET and CT images.

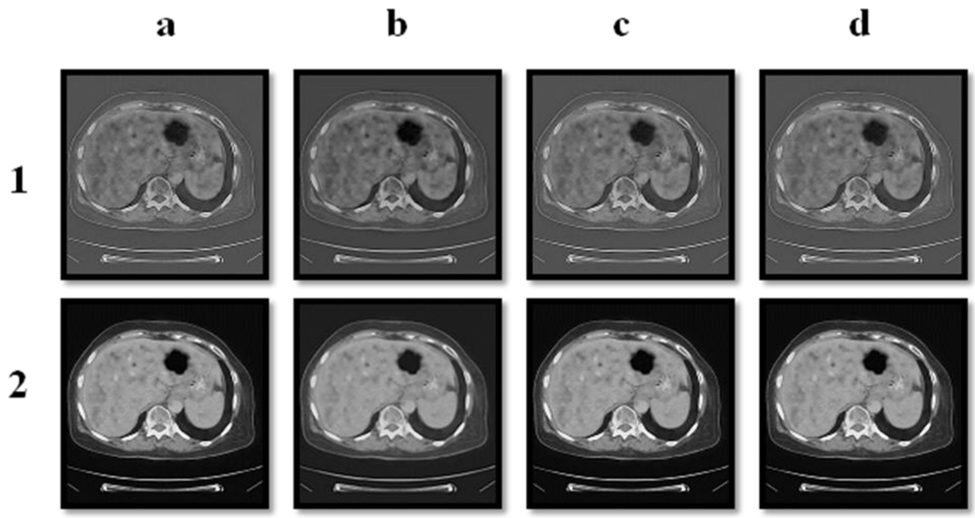

Figure 7. Data Set1: Resultant Images of WT Fusion Using Various Combination Rules 1a) SA-MAX 1b) SA-ABS_MAX 1c) SA-WA 1d) SA-WBV 2a) AWA-ABS_MAX 2b) AWA-MAX 2c) AWA-WA 2d) AWA-WBV

The quantitative analysis of the resultant images is performed using image quality metrics, image fusion metrics and error metrics as shown in table 2. The WT fusion using the newly proposed rule AWA scores the higher values for SF and ENT, which shows that it derives more information from CT and PET images than SA and also retains the contrast and sharpness. Higher values of FF, $Q^{(AB/F)}$ and MI indicates that the content extracted from the source images is more than SA rule by correlating the fused image with each of the source images, but the negative value of MI indicates that the information is not fully extracted from the source image. The error metric PFE shows that the newly proposed rule suppresses the occurrence of errors as a result of spatial reduction and expansion during the wavelet process in a better way.

Table 2. Quantitative Analysis of Data Set1

Rule	SF	ENT	FF	$Q^{(AB/F)}$	MI	PFE
SA-ABS_MAX	0.046	0.420	2.055	0.449	-11.379	63.292
SA-MAX	0.038	0.261	2.144	0.300	-12.240	61.704
SA-WA	0.046	0.419	2.060	0.448	-11.383	63.293
SA-WBV	0.046	0.419	2.059	0.448	-11.383	63.294
AWA-ABS_MAX	0.050	0.846	2.846	0.622	-8.021	47.938
AWA-MAX	0.037	0.654	2.597	0.384	-8.026	49.947
AWA-WA	0.051	0.846	2.857	0.623	-8.021	47.932
AWA-WBV	0.051	0.846	2.852	0.624	-8.022	47.972

5.2. Data Set2

The LL sub bands of the PET and CT images of data set2 are shown in Figure 8a, and 8b. Figure 8c, and 8d shows the combined approximation coefficients by using SA fusion rule and newly proposed AWA rule.

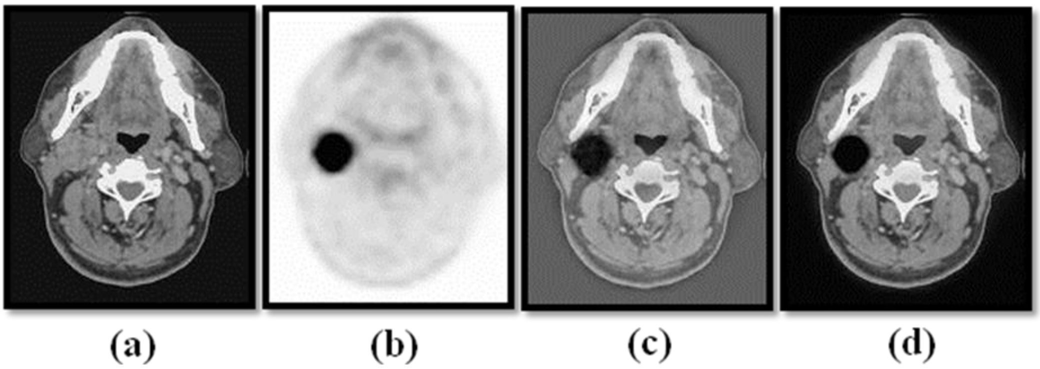

Figure 8. Data Set1 a) LL Sub Band of CT Image a) LL sub Band of PET Image c) Fused Sub Band by SA Rule d) Fused Sub Band by AWA rule

In Figure 8c, it contains both the anatomic structures from 8a, and metabolic information from 8b, but both the information are faded out. The contrast is suppressed and the entire image is not clear. Whereas the proposed AWA rule combines both the anatomic structures from 8a and metabolic information from 8b and also retains the contrast and clarity. The effectiveness of the proposed fusion rule is demonstrated by measuring the information content and clarity of the combined approximation coefficients by using the image information metrics Energy of Gradient (EOG), Standard Deviation (SD) and Shannon Entropy (ENT). If the value of the EOG is higher, the image shows better information. The SD measure the contrast of the image. The higher the contrast, clearer the image is. ENT is a statistical measure used to characterize the texture of an image. The values of EOG, SD and ENT for the fused approximation coefficients of the PET and CT images of data set 2 are given in table 3.

Table 3. Estimation of EOG, SD and ENT for the Fused Approximation Coefficients of Data Set2

Fusion Rule	EOG	SD	ENT
SA	10461190	6.2771	42.4423
AWA	14593769	6.6483	71.1160

The proposed fusion rule AWA scores higher values for EOG, SD and ENT, which shows that it is superior in terms of information content and contrast for the fusion of approximation coefficients of the CT and PET images.

Figure 9, shows the resultant fused images of data set2 for WT based image fusion using different fusion rules. In Figure 9, the Figures 1a, 1b, 1c and 1d, are the output images obtained using SA rule for approximation coefficients and ABS_MAX, MAX, WA and WBV rules for detail coefficients, respectively. In the same way, the figures 2a, 2b, 2c and 2d, are the output images obtained using AWA rule for approximation coefficients and ABS_MAX, MAX, WA and WBV rules for detail coefficients, respectively.

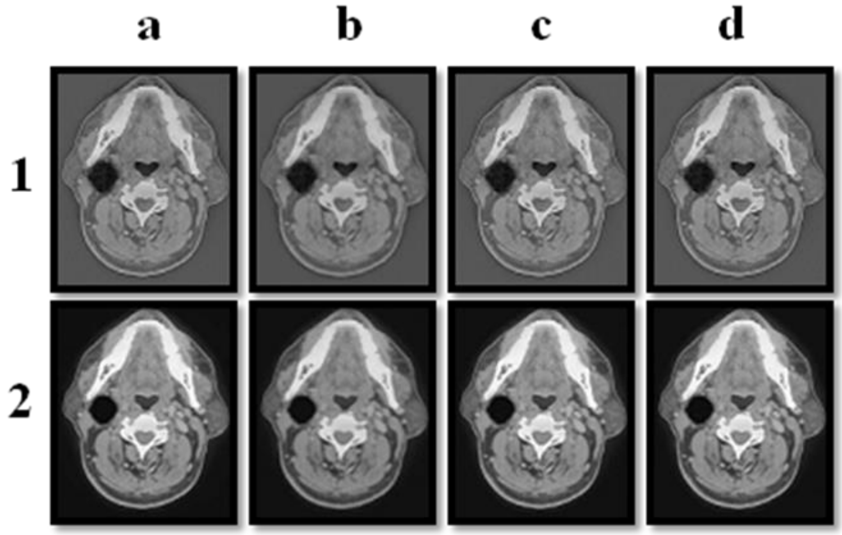

Figure 9. Data Set2: Resultant Images of WT Fusion using Various Combination Rules 1a) SA-MAX 1b) SA-ABS_MAX 1c) SA-WA 1d) SA-WBV 2a) AWA-ABS_MAX 2b) AWA-MAX 2c) AWA-WA 2d) AWA-WBV

In Figure 9, the Figures 1a, 1b, 1c and 1d, are the output images obtained using SA rule for approximation coefficients and ABS_MAX, MAX, WA and WBV rules for detail coefficients, respectively. In the same way, the Figures 2a, 2b, 2c and 2d, are the output images obtained using AWA rule for approximation coefficients and ABS_MAX, MAX, WA and WBV rules for detail coefficients, respectively.

From visual comparison, it is well known that the newly proposed adaptive weighted average rule extracts the bony structures from CT image and metabolic information from PET image instead of blind average, and the fine details such as edges are extracted from the detail coefficients effectively in such a way that the resultant fused image is rich in content as well as it retains the details such as contrast and edges.

Table 4. Quantitative Analysis of Data Set2

Rule	SF	ENT	FF	$Q^{(AB/F)}$	MI	PFE
SA-ABS_MAX	0.050	0.899	2.466	0.488	0.112	49.82
SA-MAX	0.044	0.812	2.528	0.297	-0.009	49.28
SA-WA	0.052	0.898	2.473	0.487	0.110	49.80
SA-WBV	0.052	0.898	2.473	0.487	0.110	49.80
AWA-ABS_MAX	0.056	0.967	3.532	0.635	0.254	41.17
AWA-MAX	0.043	0.922	3.170	0.377	0.253	41.46
AWA-WA	0.056	0.968	3.533	0.638	0.254	41.17
AWA-WBV	0.056	0.968	3.536	0.638	0.254	41.17

The quantitative analysis of the resultant images is performed using image quality metrics, image fusion metrics and error metrics, and is shown in table 4. The WT fusion using the newly proposed rule scores the highest values for SF and ENT, which shows that it is superior to SA in terms of contrast, sharpness and content. Higher the values of FF, $Q^{(AB/F)}$ and MI indicates that the content extracted from the source images is more than SA rule. The error metric PFE shows that the newly proposed rule suppresses the errors in a better way.

6. Conclusion

In this paper, the anatomical information from CT image and the metabolic information from PET image are effectively fused using the newly proposed Adaptive Weighted Average fusion rule (AWA). The newly proposed fusion rule is implemented for combining only the approximation coefficients of PET and CT images. The visual interpretation and quantitative analysis demonstrate that the newly proposed fusion rule combines the complementary information from the anatomical and functional images while also retaining the contrast and texture of an image. Since approximation coefficients represent the smoothed version of an original image and the CT and PET images have complementary information, this fusion rule is more appropriate for PET/CT technology. The detail coefficients contains the salient features like edges and corners in the image, and if these salient features are combined using the suitable fusion rule, the resultant fused image is rich in content with sharp edges and corners and also at fine contrast level, which helps the physician in accurate location of disease with respect to anatomical information. Even though, this fusion rule combines the approximation coefficients effectively, the calculation of adaptive weight is based on only the glucose absorption rate present in the PET image. But in practical, it also depends on other factors like arterial blood radioactivity concentration, patient's body weight, sugar level, the time interval between the intrusion of radiotracer substance and scan *etc.,* So the other factors that affect the absorption of glucose by the tissues may also be considered for accurate calculation of adaptive weight.

References

[1] T. G. Turkington, "PET imaging basics", Clinical PET-CT in Radiology", **(2010)**, pp. 21-28.
[2] C. Pohl and J. L. Van Genderen, "Review article: Multisensor image fusion in remote sensing: Concepts, methods and applications", International Journal of Remote Sensing, **(1998)**, pp. 823-854.
[3] H. B. Mitchell, "Image Fusion Theories", Techniques and Applications, Springer, **(2010)**.
[4] H. Li, B. S. Manjunath and S.K. Mitra, "Multi-sensor image fusion using the wavelet transform", IEEE, **(1994).**
[5] P. Jagalingam and A. V. Hegde, "A review of quality metrics for fused image", Aquatic Procedia, vol. 4, **(2015)**, pp. 133–142.
[6] S. Kavitha nd K. K. Thyagharajan, "A survey on quantitative metrics for assessing the quality of fused medical images", Research Journal of Applied Sciences, Engineering and Technology, vol. 12, no. 3, **(2016),** pp. 282-293.
[7] C. S, Burrus, R. A. Gopinath and H. Guo, "Introduction to wavelets and wavelet transforms: A Primer", Prentice-Hall, Inc., **(1998)**.
[8] S. Nikolov, P. Hill, D. Bull and N.Canagarajah, "Wavelets for image fusion", Computational Imaging and Vision, vol. 19, **(2001)**, pp. 213-241.
[9] Y. Yang, D. S. Park, S. Huang and N. Rao, Medical Image Fusion via an EffectiveWavelet-Based Approach, EURASIP Journal on Advances in Signal Processing, **(2010)**.
[10] H. Li, B.S. Manjunath and S.K. Mitra. Multisensor image fusion using the wavelet transform. Graphical Models and Image Processing, vol. 57, **(1995),** pp. 235–245.
[11] K. P. Indira, "Image Fusion For Pet Ct Images Using Average Maximum And Average Contrast Rules", vol.10, no.1, **(2015),** pp. 673-680.
[12] B. Shalchian, H. Rajabi and H. S. Zadeh, "Fusion of PET and CT images using wavelet transform, "Journal of Nuclear Medicine", vol. 12, no. 3, **(2009)**, pp. 238-243.
[13] P. J. Burt and R. J. Kolczynski, "Enhanced image capture through fusion", Proceedings of the 4th International Conference on Computer Vision, **(1993),** pp. 173–182.

